A Power-Efficient and Safe Neural Stimulator Using Ultra-High Frequency Current Pulses for Nerve Conduction Block

Rui Guan, Koen M. Emmer, Virgilio Valente and Wouter A. Serdijn
Section Bioelectronics, Dept. Microelectronics, Faculty EEMCS, Delft University of Technology, Delft, The Netherlands
Email: R.Guan-1@tudelft.nl, koen.emmer@gmail.com, V.Valente@tudelft.nl, W.A.Serdijn@tudelft.nl

***Abstract*—Kilohertz frequency alternating current (KHFAC) stimulation can induce fast-acting, reversible and repeatable nerve conduction block, and is a candidate therapeutic method for diseases caused by undesired neural activities, such as urinary retention. In this paper, we first show that ultra-high frequency (UHF) current pulses can also lead to successful nerve conduction block, based on simulation results using the McIntyre-Richardson-Grill (MRG) model. This model describes a myelinated axon of mammalian animals. Second, we present a prototype of a power efficient neural stimulator using UHF current pulses with active charge balancing (CB). The stimulator is built using off-the-shelf components and can be battery-powered. It uses a DC-DC boost converter without a big filtering capacitor, for generating UHF current pulses. The power efficiency of the complete system is up to 98% when testing with an equivalent circuit model of electrode tissue interface (ETI). Safety measurement results show that the electrode offset voltage can be as high as 1.3 V without charge balancing, in *in vitro* experiments with titanium electrodes in a phosphate buffered saline (PBS) solution. However, this electrode offset voltage can be successfully lowered to less than 42.5 mV, by means of negative-feedback duty cycle control of the H-bridge clock. The active CB is adopted for KHFAC stimulation for the first time.**

Keywords—nerve conduction block, ultra-high frequency (UHF) current pulses, DC-DC boost converter, active charge balancing (CB).

I. INTRODUCTION

Millions of people have painful difficulty in voluntarily urinating despite having a full bladder [1]. This is known as urinary retention. The most common treatment is to mechanically empty the bladder with intermittent self-catheterization or an indwelling catheter, which results in infections, pain and excessive healthcare costs, greatly affecting quality of life [2]. Neural modulating technologies for bladder dysfunction [3] have attracted more and more attention because of patient-tailored therapy and less side effects. One method is sacral anterior root stimulation. However, this type of stimulation therapy requires sacral posterior rhizotomy [4]. Another popular technology is relaxing the external urinary sphincter by blocking the pudendal nerves, based on the mechanism of KHFAC stimulation [4]. After the KHFAC stimulation is switched off, the external urethral sphincter can recover to its normal closure function rapidly. To the best of our knowledge, there is no specific implantable stimulator circuit design for KHFAC stimulation. For this reason, we focus on the prototype of KHFAC stimulator circuits for treatment of urinary retention, in this paper.

For implantable neural stimulators, one critical specification is the power efficiency from the dynamic power supply to the stimulation loads, as it determines the lifetime and size of the battery. Additionally, heat dissipation should be minimized to avoid any tissue damage caused by an increased temperature inside the body. To address these issues, one promising method is using a switched-mode DC-DC converter to generate UHF current pulses [5], which features the unprecedented power efficiency. It avoids the need of bulky filtering capacitors to stabilize the converter output voltage. Moreover, the stimulator can drive multiple channels simultaneously with programmable intensity and polarity, by using pulse interleaving [5].

Another important issue is safety. In order to avoid electrode degradation and tissue damage caused by irreversible Faradaic reactions at the ETI [6], any remaining offset voltage on the electrodes caused by residual charge should be within the safety window of ±50 mV [7]. In [8], a passive second order high-pass filter is used to reduce the offset voltage on the electrodes with KHFAC stimulation, but the bulky capacitors and inductors are not practical for implantable neural stimulators. Furthermore, zero mean charge of the input biphasic stimulation current cannot ensure safety because of the non-linearity of the ETI [9-10]. In [7], it talks about an active CB system using a negative feedback loop controlling amplitude of the biphasic stimulation current, which can ensure safety by measuring the electrode voltage during every stimulation cycle.

In this paper, an inductor-based DC-DC boost converter is employed to obtain a high power efficiency. The traditional large filtering capacitor is removed to reduce the number of external components, and generate UHF current pulses. Besides, it is the first time to implement active CB for KHFAC stimulation applications, by means of duty cycle control of the H-bridge clock. This negative feedback loop automatically controls the offset voltage within the safety window, by continuously monitoring voltage on the stimulation electrodes.

The rest of the paper is organized as follows: Section II introduces the working principle of UHF current pulses stimulation for nerve conduction block. The system design is presented in Section III. Section IV gives experimental results

on power efficiency and active charge balancing. This is followed by conclusions and future work in Section V.

II. UHF STIMULATION FOR NERVE CONDUCTION BLOCK

KHFAC stimulation has been shown to perform quick and reversible nerve conduction block in the MRG model that describes myelinated axons of mammalian animals, and in animal models [11-12]. However, unlike the use of UHF current pulses, kilohertz alternating constant current sources do not offer a good power efficiency [5]. In order to prove the efficacy of UHF current pulses stimulation, a simulation setup similar to the one presented in [12] was constructed, as shown in Fig. 1. Action potentials were generated at one end of the axon (Node 0). An extracellular point electrode was positioned near the middle of the axon (Node 25), and set to deliver UHF current pulses according to the pattern depicted in Fig. 2. The block frequency and amplitude for mammalian animals lie in the ranges of kilohertz and milliamp, respectively [11]. As an example, the amplitude, frequency and duty cycle of the KHFAC stimulation current were set to 30 mA, 10 kHz and 50%, respectively, with no inter-pulse delay. In reality, these parameters should be programmable within proper ranges for different patients. In order to reach the stimulation charge threshold [6], each stimulation period of 0.1 ms comprises 50 positive UHF pulses, followed by 50 UHF negative pulses. It is a compromise between UHF pulse frequency and amplitude.

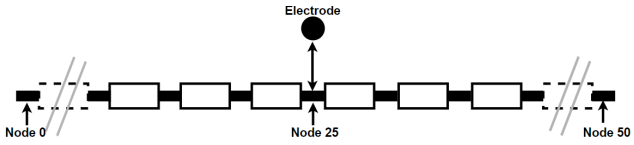

Fig. 1. A 51-node MRG model used to simulate nerve conduction block induced by UHF current pulses. Action potentials were generated at Node 0. The point electrode near Node 25 worked as block point with UHF current pulses, and the block efficiency was recorded at Node 50.

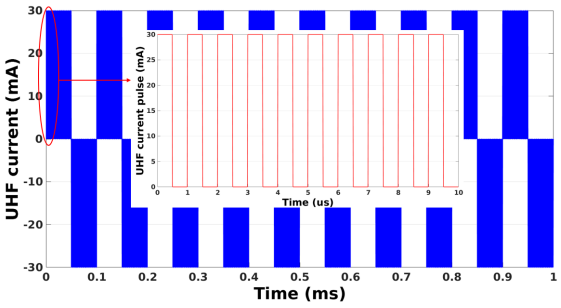

Fig. 2. Example of a KHFAC (ten periods), each period (0.1 ms) comprises of 50 positive UHF current pulses, followed by 50 negative UHF current pulses. Details of the stimulation current are shown by a zoomed-in view.

The membrane voltages at different nodes of the axon within a simulation time of 20 ms are shown in Fig. 3. The membrane voltage at the opposite end of the axon (Node 50) were stable around the resting membrane voltage after the onset response [12]. It means that there is no action potential traveling through this UHF block node. These results illustrate, for the first time, the successful nerve conduction block induced by UHF current pulses. Therefore, we design a prototype of KHFAC stimulator using UHF current pulses for treatment of urinary retention.

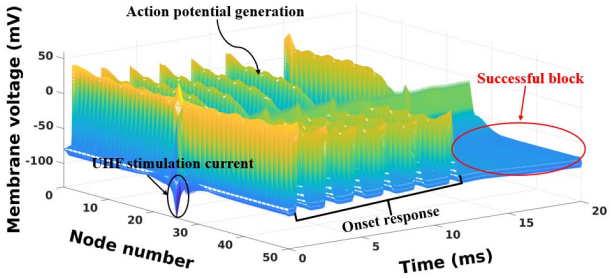

Fig. 3. Simulation results of nerve conduction block obtained from Neuron software. After the on-set response, there were no action potentials at the end of the axon, which proved that a successful nerve conduction block had been created.

III. SYSTEM DESIGN

This section describes a power efficient and safe KHFAC stimulation system design. It consists of a boost converter, an H-bridge and active CB, with single power supply.

A. Boost converter and H-bridge

The schematic of the proposed power efficient stimulator is as shown in Fig. 4. It adopts an inductor-based filter-less DC-DC boost converter generating UHF current pulses. A H-bridge is used for the generation of a biphasic stimulation current through the load from a single-ended input. The stimulation intensity can be adjusted by the duty cycle of Clk1 (D1). The durations of the cathodic and anodic phases are determined by the duty cycle of Clk2 (D2). In this design, the Clk1 and Clk2 frequencies are chosen to be 1 MHz and 10 kHz, respectively, according to the simulation results obtained in Section II.

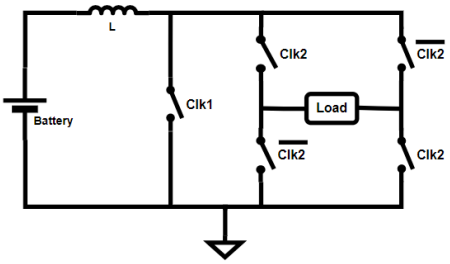

Fig. 4. Principle circuit diagram of the designed filter-less boost converter and H-bridge. Stimulation intensity can be adjusted by the duty cycle of Clk1 (D1).

B. Active charge balancing

The block diagram in Fig. 5 shows the architecture of the CB system for safety. The offset voltage, V_{os}, across the load is measured by subtracting the DC components of the voltages at both stimulation electrodes, by two 1st-order passive RC filters with a cut-off frequency of 1 Hz and a difference amplifier. The safety reference voltage, V_{ref}, is set to 0 V in this work. The proportional controller is needed for stability and accuracy of the negative-feedback loop. Finally, the amplified control

error, V_{err}, is used to adjust D2, through a voltage controlled pulse width modulation (PWM) component.

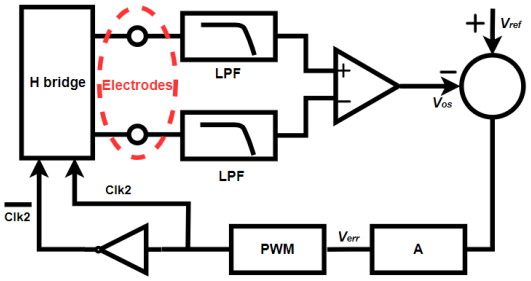

Fig. 5. System overview of the active CB loop. Safety reference V_{ref} is chosen to be 0 V in this work. A is a proportional controller. Block PWM controls the duty cycle of Clk2 (D2).

Fig. 6 illustrates the equivalent circuit model of the ETI [9], which is used for analyzing the negative feedback system in Fig.5. C_H, R_F, and R_S represent the Helmholtz double layer capacitance, the Faradaic resistance and the tissue resistance, respectively. Hence, the impedance of ETI can be expressed by Eq. 1, which has one pole and one zero. As the other control loop elements do not introduce dominant poles or zeros, and the dynamic behavior of the ETI dominates the control loop. It behaves as a first-order control system which guarantees the stability of the negative-feedback loop.

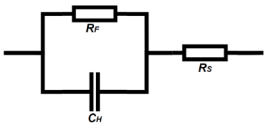

Fig. 6. Equivalent circuit model of ETI, C_H, R_F, R_S are the Helmholtz double layer capacitance, Faradaic resistance, and tissue resistance. Eq.1 describes its impedance, with one pole and one zero.

$$Z_{ETI} = \frac{sR_SR_FC_H+R_F+R_S}{sR_FC_H+1} \quad (1)$$

IV. EXPERIMENTAL RESULTS

In this section, the power efficiency of the whole system was analyzed using the equivalent circuit model of the ETI as stimulation loads, and *in vitro* experiments were conducted to measure the offset voltage with and without active CB, to validate the safety specification of this stimulator. The complete system was implemented on a printed circuit board (PCB) with discrete components.

A. Power efficiency

The power efficiency of the complete stimulation system is defined as the ratio of the power consumption on stimulation loads, P_L, and the power delivered by the energy source, P_S. The whole system power mainly consists of the power consumption on stimulation loads, active CB loop, and the MOSFET drivers for high side switches of the H-bridge. In order to measure the power efficiency with different stimulation loads, equivalent circuit model of the ETI, with C_H and R_F being 1 µF and 1 MΩ, respectively, was constructed. Measurement results with three different R_S values, of 1 kΩ, 500 Ω, and 100 Ω, were collected. P_L was calculated with the root mean square (rms) voltage on R_F and R_S. Fig. 7 shows the power delivered to stimulation load, P_L, depending on D1.

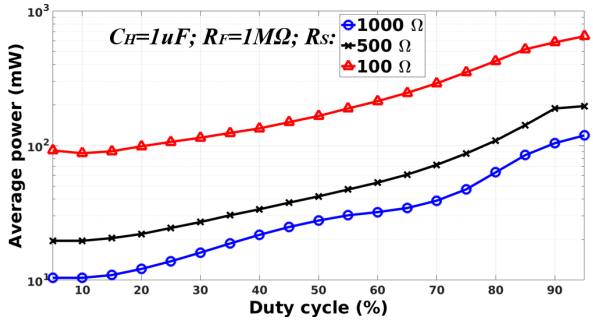

Fig. 7. Delivered average power to the equivalent circuit model of the ETI. P_L is a function of the duty cycle of Clk1 (D1). An oscilloscope (Tektronix TDS 2014C) was used to measure the root mean square (rms) voltage on R_F and R_S, for power consumption calculation.

Fig. 8 shows the measured power efficiency versus the D1 for different tissue resistances. Power from energy source was measured by a source meter (Keithley 6430). The highest power efficiency of 98% was achieved for a tissue resistance of 100 Ω and D1 of 5%. The larger the stimulation load, the less power dissipated in the load, leading to a smaller power efficiency.

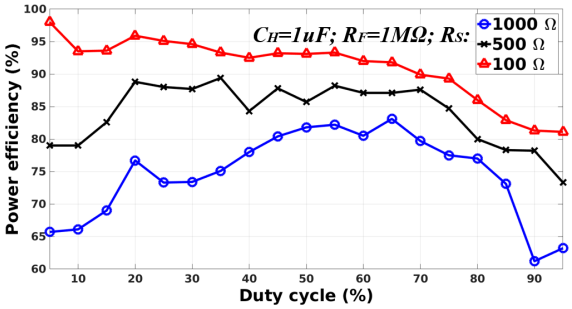

Fig. 8. Measured power efficiency using the equivalent circuit model of the ETI, with C_H = 1 uF, R_F = 1 MΩ, and three different values of R_S. The power efficiency changes with stimulation intensity and stimulation load.

B. Active charge balancing

The *in vitro* experimental setup for measuring the offset voltage on electrodes is shown in Fig. 9. A titanium electrode array in a phosphate buffered saline (PBS) solution was used. The offset voltage on the electrodes was measured by a multimeter (Hewlett Packard 34401A), with different stimulation intensities which was controlled by the duty cycle of Clk1 (D1).

First, the active CB control system was disabled. The resulting offset voltage measurement results are shown in Fig. 10. Only D1 was below 10%, the offset voltage was within the safety window of ±50 mV, but it went up to 1.3 V when D1 increased to 95%, as a result of the nonlinearity of the ETI and charge mismatch between cathodic and anodic phase. In [9], it states that nonlinearity of ETI becomes more serious with larger stimulation intensity. This charge unbalance will cause electrode corrosion and tissue damage, and charge balance control is needed for the safe implantable neural stimulator.

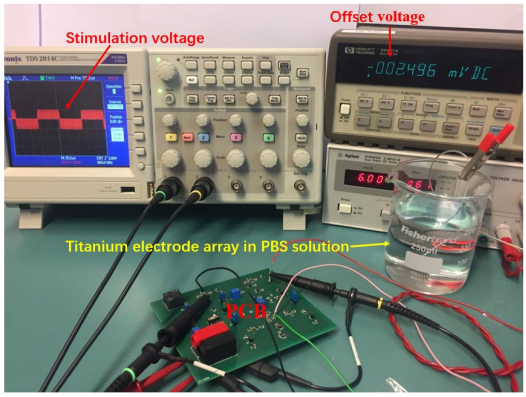

Fig. 9. *In vitro* experimental setup for validating safety of stimulator, using a multimeter (Hewlett Packard 34401A) measuring the offset voltage across titanium electrodes in the PBS solution. The whole system was implemented on PCB, powered from a power supply (Agilent E3620A). The oscilloscope (Tektronix TDS 2014C) was observing the stimulation voltage on the electrodes.

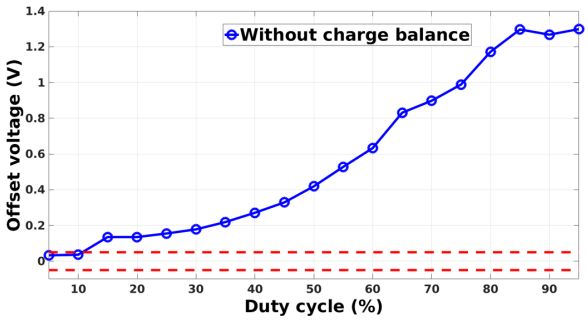

Fig. 10. Measured electrode offset voltage as a function of stimulation intensity, while CB disabled. The dashed lines indicate the safety window of ±50 mV. The duty cycle of Clk2 (D2) is 50%.

Fig. 11 shows the measured offset voltage with proportional controlled active CB enabled. It successfully stays within the safety window of ±50 mV for all different stimulation intensities. The *in vitro* results show that safety of this neural stimulator can be ensured by active CB. With the increment of stimulation intensity, the offset voltage becomes larger, leading to a bigger control error of the active CB control loop.

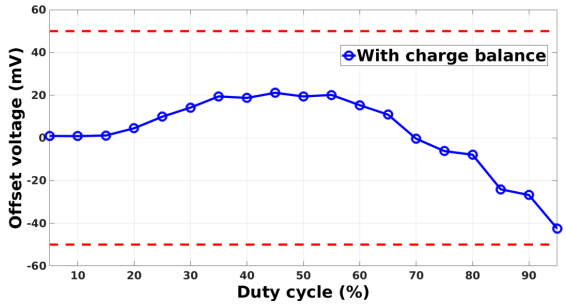

Fig. 11. Measured electrode offset voltage with active CB enabled. The offset voltage always stays within the safety window (i.e., between the dashed lines), despite varying stimulation intensity.

V. Conclusions and Future Work

This prototype demonstrates a power efficient and safe neural stimulator for nerve conduction block, employing ultra-high frequency (UHF) current pulses. The filter-less DC-DC boost converter can achieve a power efficiency up to 98%. For safety control, an active charge balancing (CB) scheme using duty cycle control of the H-bridge clock is proposed for the first time. Without active CB, the offset voltage can build up to as high as 1.3 V causing serious tissue damage. But it always stays within the safety window of ±50 mV, while active CB is working.

Future work will focus on *in vivo* experiments to verify the suitability of the proposed technique for treatment of urinary retention.

Acknowledgment

This work is in collaboration with Urologist Bertil Blok at the Erasmus Medical Center, Rotterdam, the Netherlands. The authors would like to thank Ali Kaichouhi for the technical support with PCB fabrication and measurements.

References

[1] B.A. Selius and R. Subedi, "Urinary retention in adults: diagnosis and initial management," American family physician, vol. 77, no. 5, 2008.

[2] C. R. Chapple, A. J. Wein, and N. I. Osman, "Underactive bladder," Springer, International Publishing, 2017.

[3] J. W. Lee, D. Kim, S. Yoo, H. Lee, G.H. Lee, and Y. Nam, "Emerging neural stimulation technologies for bladder dysfunctions," International neurourology journal, vol. 19, no. 1, pp. 3, 2015.

[4] H. Cai, T. Morgan, N. Pace, B. Shen, J. Wang, J.R. Roppolo, K. Horlen, P. Khanwilkar, W.C. de Groat, and C. Tai, "Low pressure voiding induced by a novel implantable pudendal nerve stimulator," Neurourology and Urodynamics, 2019.

[5] M.N. van Dongen and W.A. Serdijn, "A power-efficient multichannel neural stimulator using high-frequency pulsed excitation from an unfiltered dynamic supply," IEEE transactions on biomedical circuits and systems, vol. 10, no. 1, pp. 61-71, 2014.

[6] D.R. Merrill, M. Bikson and J.G. Jefferys, "Electrical stimulation of excitable tissue: design of efficacious and safe protocols," Journal of neuroscience methods, vol. 141, no. 2, pp. 171-198, 2005.

[7] K. Sooksood, T. Stieglitz and M. Ortmanns, "An active approach for charge balancing in functional electrical stimulation". IEEE Transactions on Biomedical Circuits and Systems, vol. 4, no. 3, pp. 162-170, 2010.

[8] M. Franke, N. Bhadra, N. Bhadra and K.L. Kilgore, "Direct current contamination of kilohertz frequency alternating current waveforms," Journal of neuroscience methods, 232, pp. 74-83, 2014.

[9] M. Sawan, Y. Laaziri, F. Mounaim, E. Elzayat, J. Corcos, and M. M. Elhilali, "Electrode–tissues interface: Modeling and experimental validation," Biomedical materials, vol. 2, no.1, pp. S7,2007.

[10] M.N. van Dongen and W.A. Serdijn , "Does a coupling capacitor enhance the charge balance during neural stimulation? An empirical study," Medical & biological engineering & computing, vol. 54, no. 1, pp. 93-101, 2016.

[11] K. L. Kilgore, and N. Bhadra, "Reversible nerve conduction block using kilohertz frequency alternating current," Neuromodulation: Technology at the Neural Interface, vol. 17, no. 3, pp. 242-255, 2014.

[12] N. Bhadra, E.A. Lahowetz, S.T. Foldes and K.L. Kilgore, "Simulation of high-frequency sinusoidal electrical block of mammalian myelinated axons," Journal of computational neuroscience, vol. 22, no. 3, pp. 313-326, 2007.